Systematic palaeontology (Vertebrate palaeontology)

# The palaeohistology of the basal ichthyosaur *Mixosaurus* Baur, 1887 (Ichthyopterygia, Mixosauridae) from the Middle Triassic: Palaeobiological implications

*La paléohistologie de l'ichthyosaure basal Mixosaurus Baur, 1887 (Ichthyopterygia, Mixosauridae) du Trias moyen : implications paléobiologiques*

Christian Kolb , Marcelo R. Sánchez-Villagra , Torsten M. Scheyer *

*Paläontologisches Institut und Museum der Universität Zürich, Karl Schmid-Strasse 4, 8006 Zürich, Switzerland*

## ARTICLE INFO

## ABSTRACT

Here, we provide the first bone histological examination of an ontogenetic series of the basal ichthyosaur *Mixosaurus* encompassing postnatal to large adult specimens. Growth marks are present in sampled humeri, a femur, a fibula, as well as in other skeletal elements (gastral ribs). Ontogenetic changes are traceable throughout stylo- and zeugopodial development, but interior remodelling and resorption deleted part of the internal growth record in the primary cortex. *Mixosaurus* humeri started as flat structures consisting of a core of endochondral woven bone and residual calcified cartilage, whereas growth continued by deposition of periosteal fibrolamellar and parallel-fibred bone. Unlike the fast-growing post-Triassic ichthyosaurs that lack growth marks, microstructural and life history data are now becoming available for a basal ichthyosaur. The high growth rate of *Mixosaurus* may indicate that higher metabolic rates characterised small, non-thunniform ichthyosaurs, as had been suggested already for post-Triassic, cruising forms.

## RÉSUMÉ

Nous rapportons ici la première étude ostéohistologique d'une série ontogénétique quasi-complète (spécimens postnatauux à adultes) de l'ichthyosaure basal *Mixosaurus*. Des stries de croissance sont visibles sur les humérus échantillonnés, ainsi que sur un fémur, un péroné et d'autres éléments du squelette (côtes gastriques). On peut suivre les changements ontogénétiques au cours du développement des stylo- et zeugopodes, mais le remodelage interne et la résorption ont en partie effacé l'enregistrement de la croissance interne dans le cortex primaire. Les humérus de *Mixosaurus* sont initialement des structures plates consistant en un noyau d'os endochondral en « sucre mouillé » et de cartilage calcifié rémanent. La croissance continue

\* Corresponding author.
*E-mail addresses:* christian.kolb@pim.uzh.ch (C. Kolb), m.sanchez@pim.uzh.ch (M.R. Sánchez-Villagra), tscheyer@pim.uzh.ch (T.M. Scheyer).

par dépôt d'os périostique fibrolamellaire et à fibres parallèles. Contrairement aux ichthyosaures post-triasiques à croissance rapide, qui ne présentent pas de stries de croissance, des données microstructurelles et d'histoire de vie sont maintenant disponibles pour un taxon basal du groupe. Le haut taux de croissance de *Mixosaurus* pourrait indiquer que les petits ichthyosaures non thunniformes étaient caractérisés par des taux métaboliques élevés, comme cela fut déjà suggéré pour les formes migrantes post-triasiques.

## 1. Introduction

The ichthyosaurs are a group of extinct reptiles with a strongly re-shaped body outline, showing numerous adaptations to a marine lifestyle. Because of their abundance and excellent fossil preservation, this lineage offers unique possibilities to get insights into the palaeobiology of a long extinct group of specialized marine vertebrates, which lacks any modern descendants (Sander, 2000). Ichthyosaurs are generally characterised by a fish- or dolphin-like body shape, a long snout and large eyes, but to date, the origins of ichthyosaurs within the amniote tree of life are still controversial (Motani, 1999). In more recent cladistic analyses, Ichthyopterygia have been repeatedly recovered as diapsid reptiles, possibly as sister group to Sauria, the clade which encompasses Lepidosauromorpha and Archosauromorpha (Motani et al., 1998; Müller, 2004).

Among Mixosauridae (Fig. 1), the genus *Mixosaurus,* erected by Baur (1887) based on the type species *Mixosaurus cornalianus* (Bassani, 1886), represents a particularly successful group of small to medium-sized ichthyosaurs (<2 m body length) restricted to the Middle Triassic (Motani, 1999). McGowan and Motani (2003) recognise five species of *Mixosaurus*, including *Mixosaurus atavus* (Quenstedt, 1852), *Mixosaurus nordenskioeldii* (Hulke, 1873), *M. cornalianus* (Bassani, 1886), *Mixosaurus fraasi* (Merriam, 1910), and *Mixosaurus kuhnschnyderi* (Brinkmann, 1998), of which *M. cornalianus* and

*M. kuhnschnyderi* are well known from the Middle Triassic of the Besano region, Italy, and from the Besano Formation of the Monte San Giorgio locality, Switzerland.

The impact of the general adaptation to the marine environment is clearly observable in the bone histology of ichthyosaurs. Whilst studies on bone histology of fossil reptiles have been done by many researchers in the past (Scheyer et al., 2010), the bone histology of marine reptiles, and especially of ichthyosaurs, is not well examined. Among others, Gross (1934), Kiprijanoff (1881) and Seitz (1907) already made useful detailed observations on the bone histology of post-Triassic ichthyosaurs (Fig. 1), such as *Ichthyosaurus, Ophthalmosaurus* and *Platypterygius.* In these works, the peculiar spongy nature of the bones was already noted. Especially Seitz (1907), who because of preservational restrictions analysed only thin-sections of ribs (and also restudied Kiprijanoff's original sections), mentioned that the primary bone tissue houses not only primary vascular canals and osteons but is also subject to secondary remodelling. Gross (1934) further encountered primary and secondary osteons and larger resorption bays in a section of a lower jaw of *Ichthyosaurus* sp. and in the rib of *Ophthalmosaurus icenicus.* More recently, de Buffrénil and Mazin (1990) gave a comparative account on the bone histology of the ichthyosaurs *Stenopterygius* and *Ichthyosaurus*, as well as the Early Triassic *Omphalosaurus*, an enigmatic taxon whose systematic position is still under debate (Motani, 2000; Sander and Faber, 2003). de
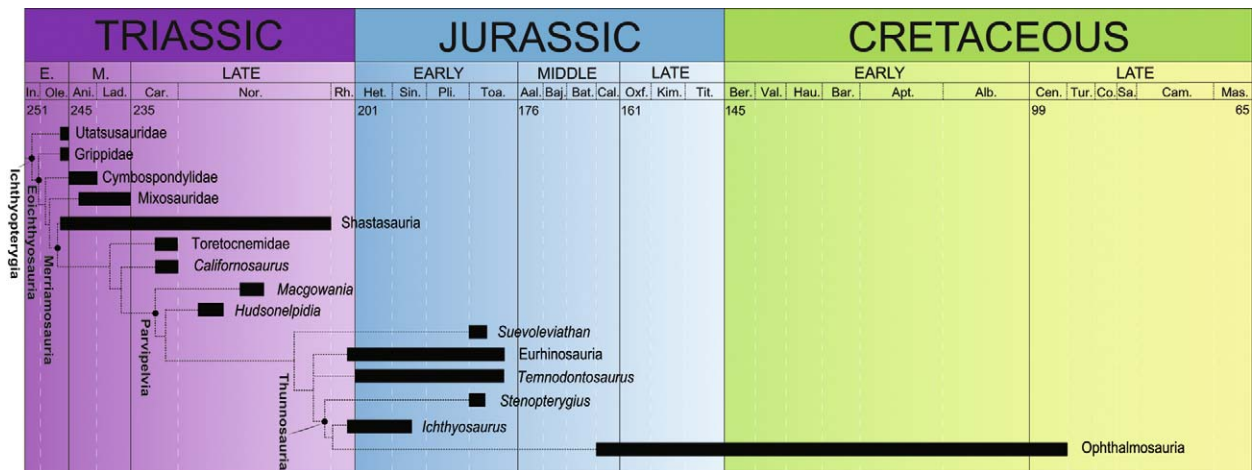


**Fig. 1.** Simplified time-calibrated cladogram (modified from McGowan and Motani, 2003; Motani, 2005; Walker and Geissman, 2009 [GSA 2009 Geologic Time Scale]) showing the interrelationships of the Ichthyopterygia and the position of the Mixosauridae within the clade.
**Fig. 1.** Cladogramme simplifié (d'après McGowan et Motani, 2003 ; Motani, 2005 ; Walker and Geissman, 2009 [GSA 2009 Geologic Time Scale]) montrant les relations entre les Ichthyopterygia et position des Mixosauridae au sein du clade.
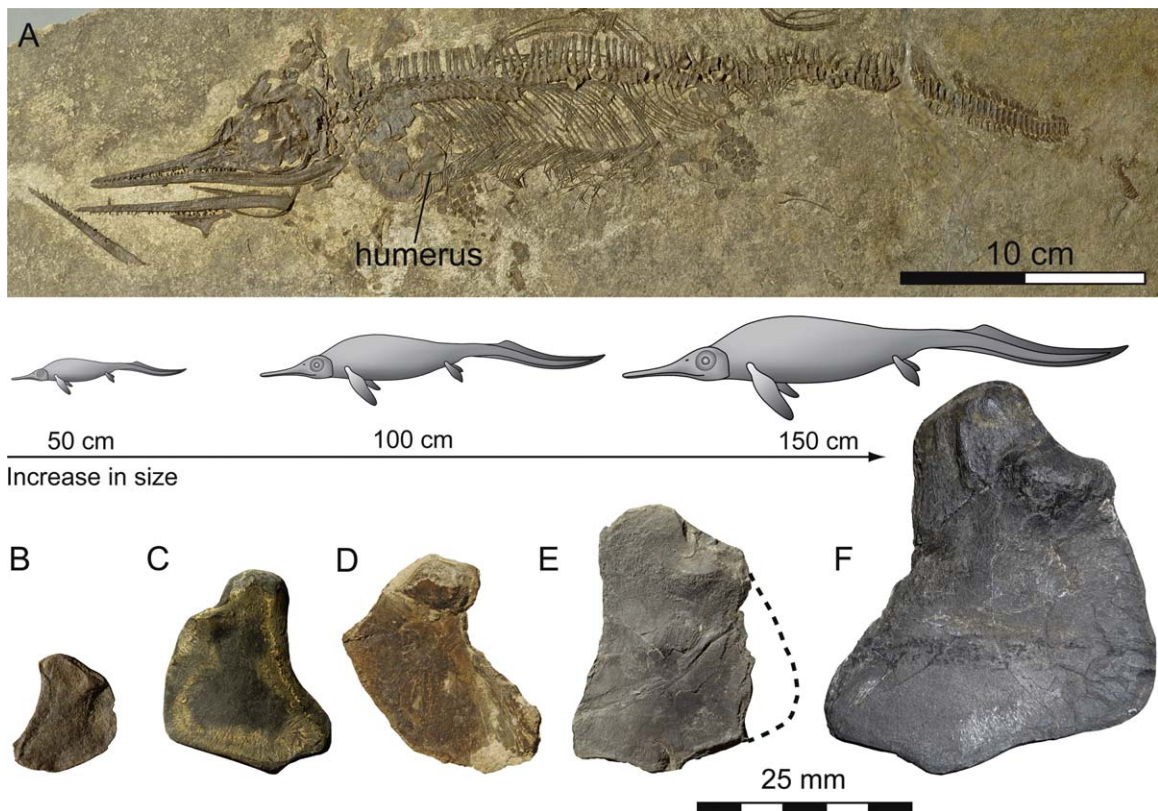
**Fig. 2.** Sampled humeri of *Mixosaurus* (Middle Triassic, Monte San Giorgio, Switzerland). Mark the arrow (time line) and mixosaur sketches showing the increase in body size of the sampled specimens. Note that the sketches do not show allometric changes throughout ontogeny. A. Smallest sampled individual of *Mixosaurus* (PIMUZ T 77). B. Small left humerus, ventral view (PIMUZ T 77). C. Right humerus, ventral view (PIMUZ T 2046). D. Distorted and crushed left humerus, dorsal view (PIMUZ T 1296). E. Distorted and crushed left humerus, ventral view (PIMUZ T 2388). Note that the anterior flange has broken off prior to sampling. F. Large left humerus, ventral view (PIMUZ T 5844).

**Fig. 2.** Humérus échantillonnés de *Mixosaurus* (Trias moyen, Monte San Giorgio, Suisse). Remarquez la flèche (axe temporel) et les croquis indiquant l'augmentation de taille des spécimens étudiés. Notez que les croquis ne montrent pas de changements allométriques pendant toute l'ontogenèse. A. Plus petit individu de *Mixosaurus* échantillonné (PIMUZ T 77). B. Petit humérus gauche, vue ventrale (PIMUZ T 77). C. Humérus droit, vue ventrale (PIMUZ T 2046). D. Humérus gauche tordu et écrasé, vue dorsale (PIMUZ T 1296). E. Humérus gauche tordu et écrasé, vue ventrale (PIMUZ T 2388). Notez que le flanc antérieur s'est brisé avant l'échantillonnage. F. Gros humérus gauche, vue ventrale (PIMUZ T 5844).

Buffrénil and Mazin (1990) showed that in bones of juvenile specimens of these ichthyosaur taxa, woven-fibred tissue was predominately deposited as well vascularised spongy bone. More compact primary bone was then subsequently deposited in older specimens before being extensively remodelled into cancellous tissue. *Mixosaurus*, on the other hand, a taxon which due to its intermediate body plan (sensu Motani, 2005) between the more basal (Early-Middle Triassic) eel-shaped and the clade of younger (post-Triassic) dolphin-shaped ichthyosaurs represents a key taxon of ichthyosaur evolution, had not been studied yet.

In this present work we describe and interpret the histological structures observed in the bones of *Mixosaurus* in comparison with that of post-Triassic ichthyosaurs. Conclusions are drawn on the implications of the observed microstructures for the palaeobiology of these highly adapted marine reptiles.

## 2. Material and methods

Various bones of the well identifiable genus *Mixosaurus* from the collections of the Palaeontological Institute and Museum of the University of Zurich were sampled. All specimens were recovered from the Middle Triassic series of Monte San Giorgio, Ticino, Switzerland. First, a series of five humeri of *Mixosaurus* was sectioned, including a humerus belonging to a very small, presumably postnatal individual (PIMUZ T 77) of about 50 cm in body length (Fig. 2A, B), three intermediate-sized specimens of 100–120 cm body length (PIMUZ T 1296, T 2046, T 2388; Figs. 2C-E), as well as a large specimen of about 150 cm body length (PIMUZ T 5844; Fig. 2F). Estimates of body length, i.e. snout-tail length, are based on comparisons with complete skeletons of *Mixosaurus* housed in the Palaeontological Museum of the University of Zurich. Moreover, various bones of the zeugo- and autopodium of PIMUZ T 2046 could be sampled. These include a femur, a fibula, an ischium, one ulna, as well as two phalanges. Additionally, it was possible to section one scapula (PIMUZ T 5844) along with rib- and gastral rib fragments (PIMUZ T 1296, T 2046).

After formatting of the bone-bearing rock samples, thin sections were produced. Following standard procedures, the samples were coated and impregnated with epoxy resin (Araldite) prior to sawing and grinding. The long bones,
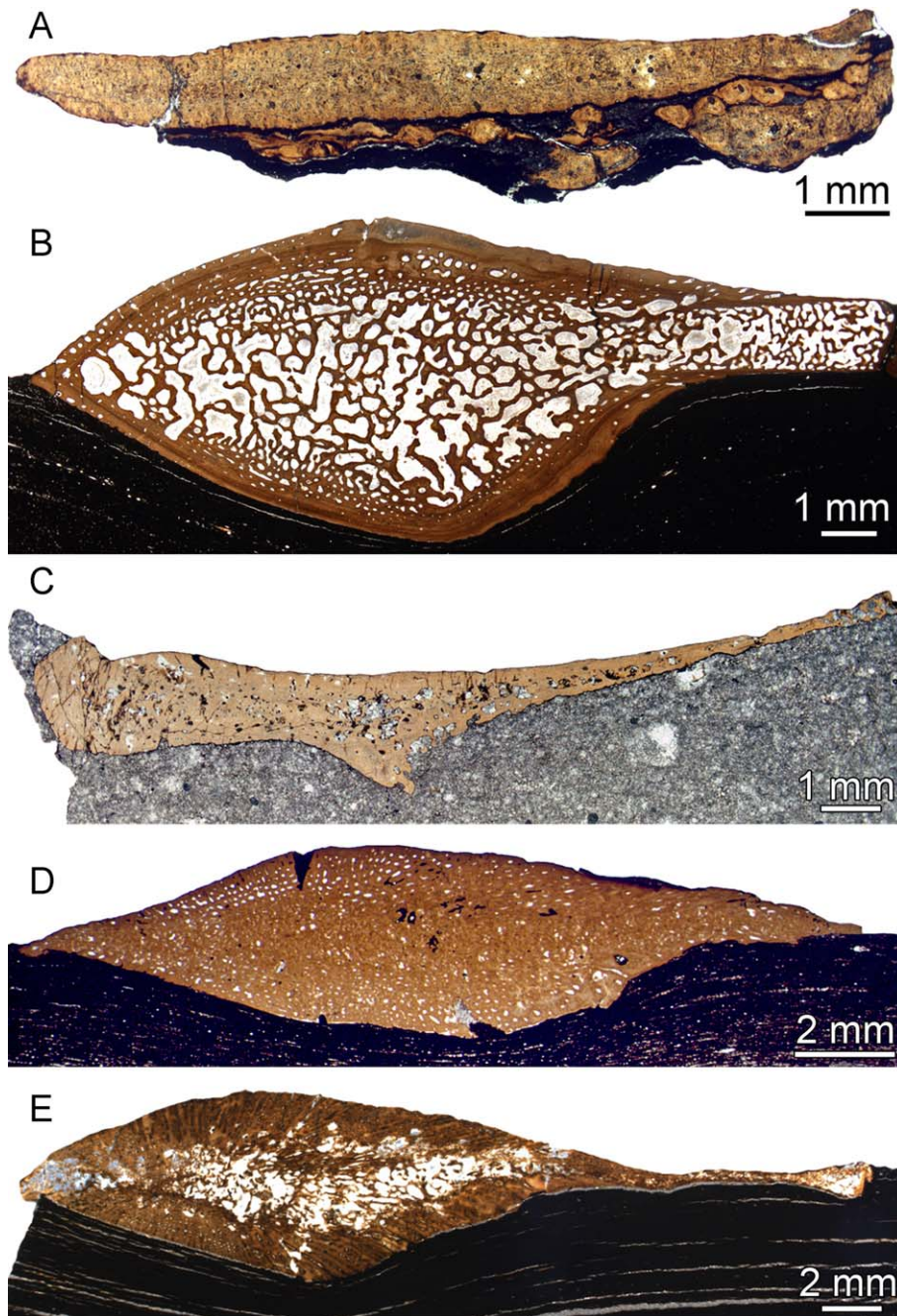
**Fig. 3.** General aspects of transverse thin-sections of humeral shafts. A. PIMUZ T 77. B. PIMUZ T 2046. C. PIMUZ T 1296. D. PIMUZ T 2388. E. PIMUZ T 5844. Note the good preservation of T 2046 (B), in contrast to the compacted specimens PIMUZ T 1296 (C) and PIMUZ T 2388 (D). Anterior is to the right.
**Fig. 3.** Aspect général des lames minces transverses des fûts huméraux. A. PIMUZ T 77. B. PIMUZ T 2046. C. PIMUZ T 1296. D. PIMUZ T 2388. E. PIMUZ T 5844. Notez la bonne préservation de T 2046 (B), a contrario des spécimens compactés PIMUZ T 1296 (C) et PIMUZ T 2388 (D). La face antérieure est à droite.

the ulna and the phalanges were transversely sectioned in the middle of the shaft whereas the ischium was sectioned along its smallest width. Sections were observed by standard light microscopy (normal transmitted and polarized light) using a Leica DM2500 M composite microscope. A Leica DFC 420 °C digital camera was used for taking micrographs. Specimens and sections are housed in the collections of the Palaeontological Institute and Museum of the University of Zurich.

### 2.1. Institutional abbreviations

**PIMUZ**: Paläontologisches Institut und Museum, Universität Zürich, Switzerland.

## 3. Results

In the following part, the main observations in the bone histology of *Mixosaurus* will be described. The histology of the ontogenetic series of humeri will be described first from the smallest to the largest specimen, followed by the histological description of the additionally sampled skeletal elements. Besides the histological features, several outer anatomical and microstructural ontogenetic changes characterise humeral growth in *Mixosaurus*. These changes include an overall increase of periosteal bone leading to a smoother bone surface, a decrease of internal vascular patterns being visible externally, and the development of a more angular bone shape with more distinct articulation facets. The length to width ratio, on the other hand, stays nearly constant throughout humeral growth.

### 3.1. Histological description of developmental series of humeri

All sampled humeri (Fig. 3) show cortical fibrolamellar bone locally substituted with parallel-fibred bone. Osteocyte lacunae with a mostly long-oval outline are present in internal woven bone as well as in the cortex. The primary osteons, which can be best observed in the primary matrix of fibrolamellar bone, show a concentric arrangement of lamellar bone which is, however, not clearly visible in every case.

The humerus of the postnatal specimen PIMUZ T 77 (Fig. 3A) has a proximodistal length of 14 mm. It shows a core of endochondral woven bone with residual calcified cartilage, which is surrounded by periosteal fibrolamellar bone (Fig. 4A). Towards the anterior flange, the amount of calcified tissue appears to increase interiorly, because of the reduced thickness of the surrounding cortical bone. The rim of the flange is capped by calcified cartilage. Vascularisation of the bone is generally low. It was possible to identify one line of arrested growth (LAG) basically encompassing the woven bone core, indicating that the specimen was in its second year of life.

Humerus PIMUZ T 2046 (Fig. 3B) has a proximodistal length of 24 mm. It is the best preserved specimen sampled, which shows almost no compaction. In the main shaft region, the cortex consists of fibrolamellar bone. Nine to ten LAGs are countable in the cortical tissue

(Fig. 4B). However, approximately three LAGs have been lost due to resorption and remodelling processes. Towards the anterior flange, the cortex is composed of parallel-fibred bone (Fig. 4C). The interior of the bone shows strong resorption in its deeper parts, whereas the trabeculae are at various stages of remodelling into secondary lamellar bone (Fig. 4D). Locally, remains of woven-fibred bone associated with calcified cartilage are still observable between the resorption bays. The anterior margin of the anterior flange shows a cap of cartilage (Fig. 4E, F).

Humerus PIMUZ T 1296 (Fig. 3C), having a proximodistal length of 23 mm, is strongly crushed and distorted and does not show a good growth record. This specimen histologically resembles PIMUZ T 2046, but it has a condensed core of crushed trabecular bone surrounded by cortical fibrolamellar bone. Sharpey's fibres are present in some areas of the dorsal part of the cortex (Fig. 4G).

The proximodistal length of PIMUZ T 2388 (Fig. 3D) with 32 mm indicates a specimen of at least intermediate to large size. Strikingly, the diaphyseal shaft region of the bone appears almost compact in cross section. However, this "compactness" results from severely crushed cancellous bone, visible as small irregularly arranged trabecular fragments of lamellar bone, filling up most of the endosteal vascular spaces. Due to this compaction the overall dorsoventral thickness of the shaft of PIMUZ T 2388 (max. 3.8 mm) measures only about 65 % of the shaft thickness of PIMUZ T 2046 (max. 5.8 mm). The outer cortex of the main shaft region is composed of fibrolamellar bone (Fig. 4H) with radially arranged primary osteons, whereas the compacta of the anterior flange consists of parallel-fibred bone. Sharpey's fibres are most prominent in the ventral compacta of the posterior shaft region.

The largest specimen is PIMUZ T 5844 (Fig. 3E); with a proximodistal length of 47 mm it has a dorsoventral thickness of the shaft of max. 6.3 mm, indicating that this specimen is also strongly compacted, as is confirmed by the histology of the specimen. The interior cancellous parts of the bone appear again quite compact, because of collapsed trabeculae filling up the vascular spaces. Otherwise this humerus shares histological features with PIMUZ T 2388, including the radial arrangement of primary osteons, the distribution of fibrolamellar and parallel-fibred tissues in the cortex, as well as the presence of Sharpey's fibres in the ventral cortex of the posterior shaft region. LAGs (Fig. 4I) are only locally preserved in the cortical tissue and hard to trace, which makes a reliable count difficult. However, taking a conservative approach, it was still possible

**Fig. 4.** Bone histology of the *Mixosaurus* humeri sampled. A. Close-up of the bone centre of PIMUZ T 77 in polarized (left) and normal light (right). White arrows mark the interior core of woven bone and calcified cartilage (lighter colour), surrounded by fibrolamellar bone. B. Close-up of the tip of the humerus PIMUZ T 2046 showing centripetally progression of erosion bays (EB) and lines of arrested growth in the cortical bone. C. Primary cortex of PIMUZ T 2046 in polarized light showing parallel-fibred bone between primary osteons. D. Cancellous and compact bone of PIMUZ T 2046 with areas of parallel-fibred bone (lower half of the image) and woven-fibred, as well as secondary lamellar bone (upper half of the image). E. Cartilage cap at the anterior flange margin of PIMUZ T 2046 in normal light. F. Cartilage cap of PIMUZ T 2046 in polarized light with lambda compensator. Note that the photograph shown in (E) and (F) was rotated 90 degrees anti-clockwise compared to Fig. 3B for technical reasons. G. Posterior region of diaphysis (PIMUZ T 1296) in polarized light with lambda compensator. The white arrow to the left indicates the crushed area of the bone. The arrow to the right indicates Sharpey's fibres (Shf, blue colours) inserting into the compact bone (yellow-orange colours). H. Cortex of PIMUZ T 2388 in polarized light consisting of fibrolamellar bone. I. Primary cortex of PIMUZ T 5844 showing typical features of the cortex of *Mixosaurus* humeri as fibrolamellar bone, primary osteons, and LAGs (lines of arrested growth) as indicated by white arrows. J. Anterior region of PIMUZ T 5844 in normal light, showing a close-up of the flange region and the cartilage cap. Note that internal bone structures have largely collapsed.
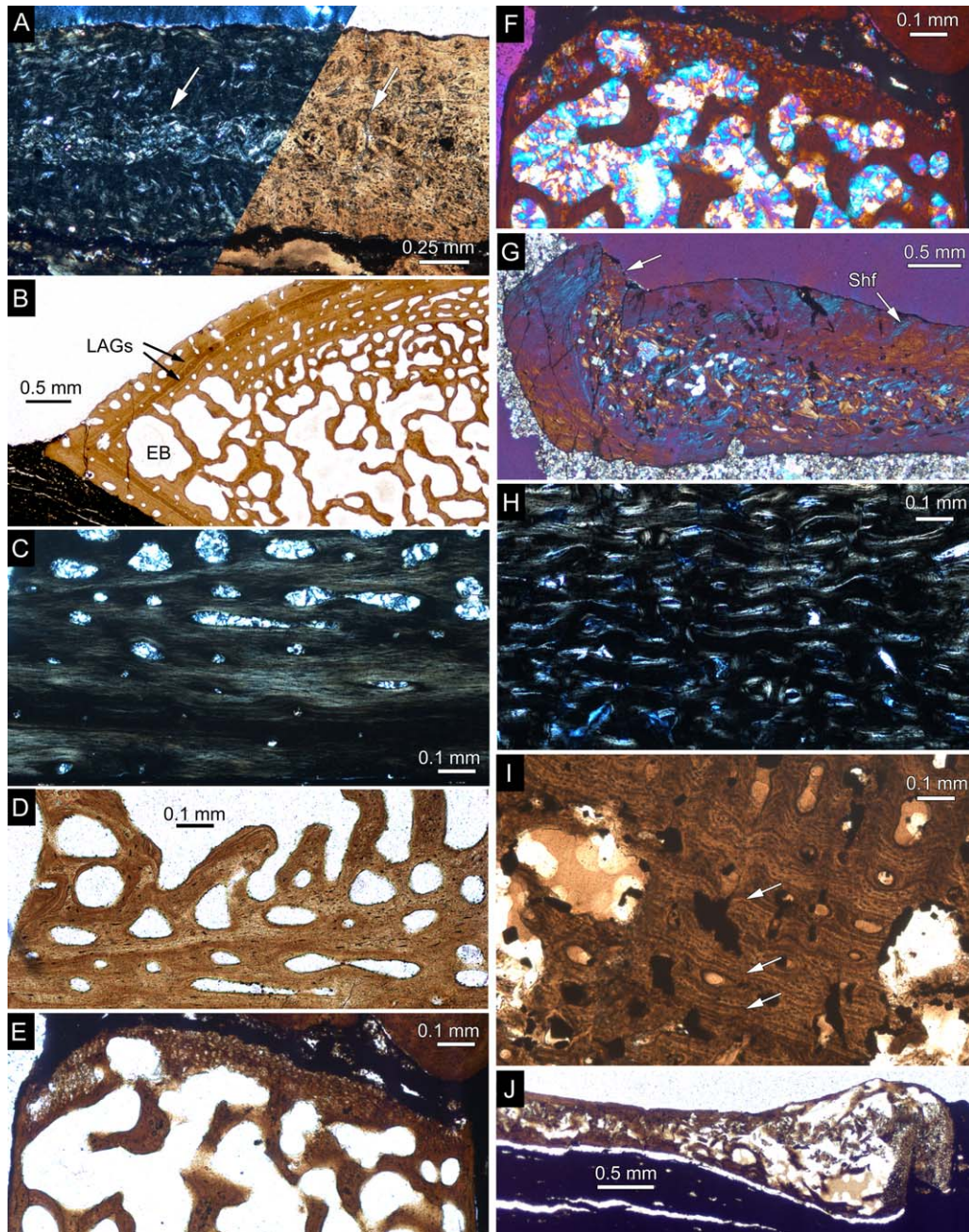
**Fig. 4.** Histologie osseuse des humérus échantillonnés de *Mixosaurus*. A. Vue rapprochée du centre osseux de PIMUZ T 77 en lumière polarisée (gauche) et naturelle (droite). Les flèches blanches marquent le noyau interne d'os en 'sucre mouillé' et de cartilage calcifié (couleur plus claire), entouré d'os fibrolamellaire. B. Vue rapprochée de la tête de l'humérus PIMUZ T 2046 montrant la progression centripète des baies d'érosion (EB) et des lignes d'arrêt de croissance dans la corticale. C. Cortex primaire de PIMUZ T 2046 en lumière polarisée montrant l'os à fibres parallèles entre les ostéons primaires. D. Os spongieux et compact de PIMUZ T 2046 avec des zones d'os à fibres parallèles (partie basse de l'image), d'os fibreux, ainsi que des zones d'os lamellaire secondaire (partie haute). E. Bouchon cartilagineux sur le bord du flanc antérieur de PIMUZ T 2046 en lumière naturelle. F. Bouchon cartilagineux de PIMUZ T 2046 en lumière polarisée avec compensateur lambda. Notez que, pour des raisons techniques, la photo a été tournée de 90 degrés. G. Région postérieure de la diaphyse (PIMUZ T 1296) en lumière polarisée avec compensateur lambda. La flèche blanche sur la gauche indique la zone écrasée de l'os. La flèche sur la droite indique les fibres de Sharpey (Shf, en bleu) s'insérant dans l'os compact (en jaune-orange). H. Cortex d'os fibrolamellaire de PIMUZ T 2388 en lumière polarisée. I. Cortex primaire de PIMUZ T 5844 montrant les attributs typiques du cortex des humérus de *Mixosaurus* : os fibrolamellaire, ostéons primaires, et lignes d'arrêt de croissance (LAGs) tels qu'indiqués par les flèches blanches. J. Région antérieure de PIMUZ T 5844 en lumière naturelle, montrant une vue rapprochée du flanc et du bouchon cartilagineux. Notez que les structures osseuses internes sont en grande partie effondrées.

to count 12 LAGs in the dorsal and ventral cortices of the mid-diaphyseal shaft region of the humerus. Taking into account that zones might have been larger in the faster growing juveniles, it is assumed that three to four LAGs have been lost through internal remodelling and resorption. Based on these assumptions, the largest individual investigated might have reached an age between 15 and 16 years. The cartilage cap (Fig. 4J) in the anterior flange is strongly developed in this humerus.

### 3.2. Histological description of additional skeletal elements

With the exception of a scapula, which belongs to PIMUZ T 5844, all of the additional specimens sampled come from PIMUZ T 2046. Based on convergent morphologies, especially of their semi-circular shaft areas, the microstructures of the femur, fibula and scapula will be described together in one section. Similarly, the flat bone morphology of the ulna and the ischium exhibit very similar histologies.

The femur (Fig. 5A) and the fibula (Fig. 5B) have a proximodistal length of 11 mm, whereas the femur shaft is slightly larger in diameter. The deeper cortical layers of both bones show fibrolamellar bone tissue, whereas the more superficial cortical layers are composed of parallel-fibred bone. The cortex of the scapula (PIMUZ T 5844) is essentially similar to that of the femur and fibula but is more variable in thickness. Osteocyte lacunae are more round-shaped in the fibrolamellar bone, whereas they are more flattened in the parallel-fibred tissue of the outer cortex. Sharpey's fibres extend extensively into all parts of the cortices, often obscuring the primary periosteal bone tissues. Primary osteons are arranged in radial rows in the outer parts of the cortices. The interior parts of the bones are strongly cancellous, with the trabeculae showing various stages of resorption and remodelling. The trabeculae in the fibula can be extremely thin. The primary bone tissue between the resorption bays consists of woven-fibred bone and residual calcified cartilage. Similar to the growth record count in the humerus, about 10 LAGs are visible in the cortices of both the femur and fibula.

The ulna (Fig. 5C) has a proximodistal length of 16 mm; the ischium (Fig. 5D) only 12 mm. Both elements have a compact cortex of parallel-fibred bone, variable in thickness, surrounding cancellous bone. In the ulna, the cortical bone, which is vascularised by scattered primary osteons, is thickest at the anterior margin and wedges out towards the posterior rim of the bone, which itself is capped by calcified cartilage. In the ischium, the anteromedial margin is concave in cross-section and also composed of calcified cartilage. In both bones, Sharpey's fibres are most conspicuous in the thickened cortical parts, where they inserted mostly perpendicularly into the primary bone tissue. Ten LAGs are countable throughout the cortex in both bones. Isolated larger erosion bays and scattered secondary osteons are found especially in the anterior part of the cortex. The cancellous bone consists of thin trabeculae, which often preserve a core of primary cartilaginous tissue.

The two phalanges sampled show periosteal parallel-fibred bone dorsally and ventrally at the bone centre, whereas the anterior and posterior parts of the bone are cancellous, consisting of primary trabeculae, which are successively remodelled (Fig. 5E). The anterior and posterior margins are covered by calcified cartilage caps. The growth record is best preserved at the cortex of the bone centre, showing nine to 10 LAGs.

Several small circular, semi-circular or bean-shaped bones, interpreted to be either ribs or gastral ribs, were sampled. Especially the gastralia, which usually lack a central marrow cavity or vascularisation, are well suited for growth record counts. The cores of the gastralia consist of a small amount of woven bone and calcified cartilage, surrounded by layers of parallel-fibred or lamellar-zonal bone. In the case of a gastral rib lying adjacent to the humerus of PIMUZ T 2046, 13 LAGs were counted (Fig. 5F). In the ribs, a large central marrow cavity is present, making them less suitable in this regard.

## 4. Discussion and conclusions

As revealed by the new data on *Mixosaurus*, the bone histology of the different bone samples is rather uniform, with changes in bone tissue types being mostly related to the different dimensions and shapes of the samples. Differences in the bone deposition rates thus appear to correlate with the overall size of the bone, in that the thickest and largest bones (i.e., humeri) show extensive woven and fibrolamellar tissue. Other limb elements (e.g. femur, fibula) show less fibrolamellar and prevalently parallel-fibred tissue, whereas the thinnest elements (e.g. ribs and gastralia) exclusively show parallel-fibred or lamellar-zonal tissue. The well-documented presence of parallel and coarse Sharpey's fibres in the ventral compacta of the posterior humeral shaft further indicates a strong muscular or tendinous region of insertion, presumably used for front limb retraction in steering.

New data on *Temnodontosaurus* (Fig. 5G; SMNS 50329) are consistent with data of de Buffrénil and Mazin (1990) that long bones of geologically younger thunniform ichthyosaurs overall show spongy cancellous tissue, as is typically encountered in vertebrates adapted to open marine conditions (Ricqlès and de Buffrénil, 2001). Unlike the geologically younger ichthyosaur clade, however, all *Mixosaurus* bones sampled reveal a good growth record (i.e. LAGs) in their cortical bone tissue. Similarly to the condition in *Mixosaurus*, LAGs appear to be present in the basal ichthyosaur *Utatsusaurus* from the Lower Triassic Osamu Formation of Japan (Nakajima, 2009) and in *Omphalosaurus* from the Lower Triassic of Spitsbergen (de Buffrénil and Mazin, 1990). An external fundamental system, i.e. a closely spaced series of LAGs at the periosteal margin indicating cessation of growth, as was briefly noted for most bones of *Utatsusaurus* by Nakajima (2009), was not found in *Mixosaurus*.

The compacta of *Mixosaurus* bones remain usually well developed throughout life, because the imbalance between bone absorption and deposition, especially the high remodelling rates of older individuals found in cruising post-Triassic ichthyosaurs, is not pronounced. As such, the bone histology fits with other morphological
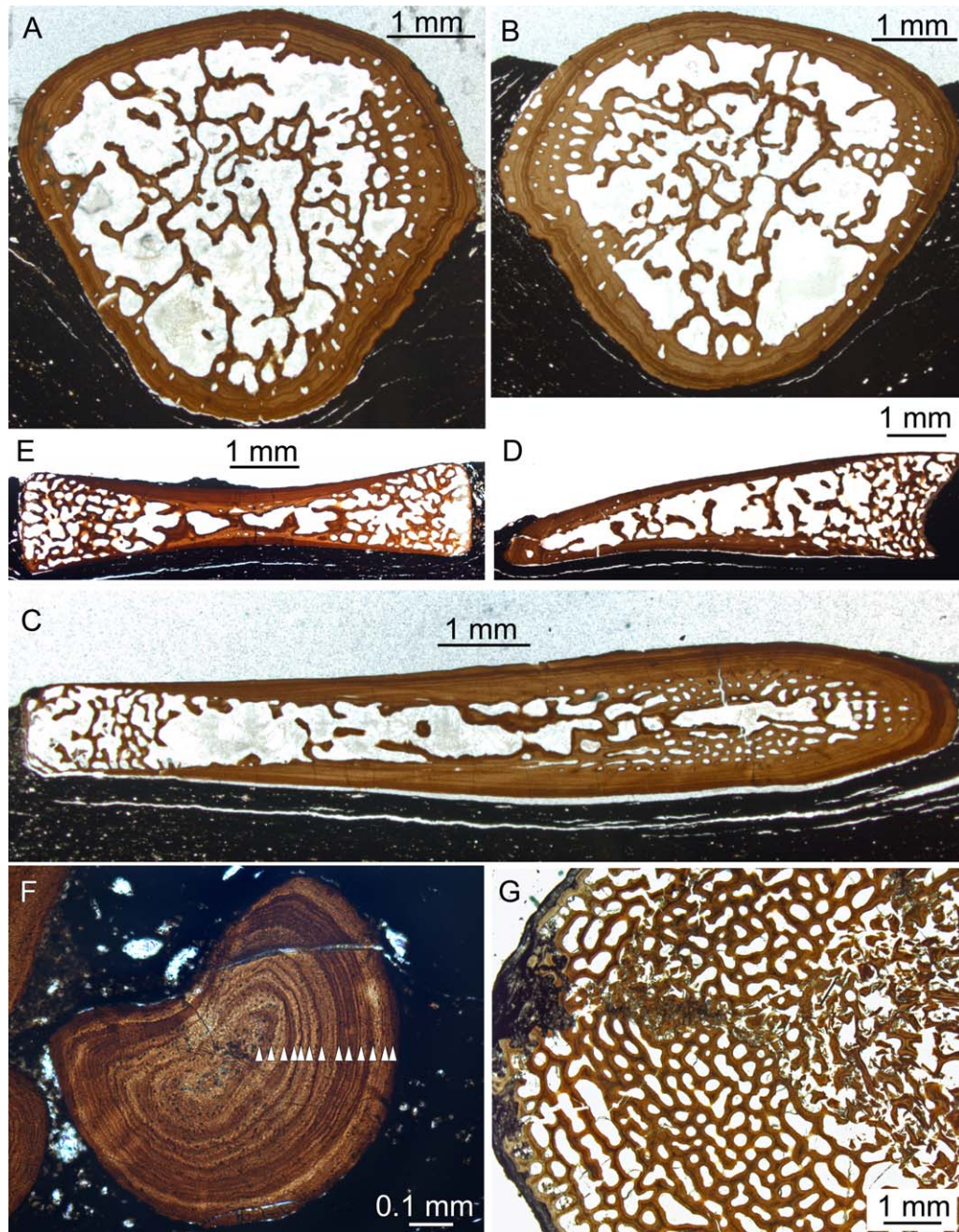
**Fig. 5.** General aspects of transverse sections of additional sampled bones of *Mixosaurus*. Specimens in (A–F) belong to PIMUZ T 2046. A. Femur. B. Fibula. C. Ulna. D. Ischium. E. Phalanx. F. Gastral rib showing 13 incremental growth circles (white triangles) consisting of zones of bone growth, annuli and LAGs. G. General texture of the cortex of *Temnodontosaurus* (Lower Jurassic, Holzmaden, Germany) in humerus SMNS 50329 showing collapse structures of the cancellous bone tissue in its centre.

**Fig. 5.** Aspect général de sections transverses d'autres os de *Mixosaurus*. Les spécimens (A–F) appartiennent à PIMUZ T 2046. A. Fémur. B. Fibula. C. Ulna. D. Ischion. E. Phalange. F. Côte gastrique montrant 13 cercles de croissance incrémentale (triangles blancs) correspondant aux zones de croissance osseuse, aux annulus et aux LAGs. G. Texture générale du cortex de *Temnodontosaurus* (Jurassique inférieur, Holzmaden, Allemagne) dans l'humérus SMNS 50 329 présentant des structures d'effondrement du tissu de l'os spongieux en son centre.

traits (i.e., non-thunniform body shape lacking well developed back– and tail fins; retention of five-fingered limbs modified in paddles with moderate polyphalangy) which characterise *Mixosaurus* as a near-shore or shelf dweller that did not venture frequently into open or deep marine environments. Note, however, that *Mixosaurus* lacks histological specialisations such as osteosclerosis or pachyostosis (Houssaye, 2009), which occur frequently in tetrapods living in shallow-water or near-shore habitats.

Caldwell (1997, 2002) pointed out that there is a proximal to distal and postaxial to preaxial perichondral bone loss in ichthyosaurs and plesiosaurians. Showing the forelimb of *M. cornalianus*, he noted the loss to occur first at the postaxial margin of the ulna, followed by the postaxial margin of the fifth metacarpal (continued by the postaxial margins of the proximal phalanges of the fifth digit) prior to the loss at the preaxial and postaxial margins of the first metacarpal (continued by the preaxial margins of the proximal phalanges of the first digit). However, as can be seen here in the histological description of the developmental series of humeri of *Mixosaurus*, the margin of the anterior (= preaxial) flange of the humeri is always capped by cartilage only, indicating also a perichondral bone loss at this position. While the proximodistal direction of bone reduction appears to be retained, the postaxial to preaxial shift proposed by Caldwell (1997, 2002) is not found in *Mixosaurus*. Therefore, *Mixosaurus*, at least in the forelimb, seems to show a divergent pattern of periosteal bone reduction, in comparison to the other ichthyosaurs.

To better understand the evolution of the dolphin-like body plan of the cruising post-Triassic ichthyosaurs (i.e., the ichthyosaur "crown"), it is important to study the palaeobiology and ecology of the more basal taxa (i.e., "stem" ichthyosaurs), to elucidate how traits evolved in this lineage. In summary, both the outer morphology and the bone microstructures of *Mixosaurus* show an intermediate state between the eel-shaped utatsusaurids or other basal eoichthyosaurians, and the more highly nested parvipelvian ichthyosaurs (Fig. 1). The *Mixosaurus* data confirm the presence of high growth rates, as expressed by the deposition of fibrolamellar bone tissue, at least in the larger, massive skeletal elements, such as the humeri, throughout ontogeny. It seems thus plausible that higher metabolic rates (as precondition for homeothermy), which were postulated to be present already in the large post-Triassic cruising ichthyosaurs and in *Omphalosaurus* (de Buffrénil and Mazin, 1990; Motani, 2010), were also present in the small non-thunniform *Mixosaurus*.

## References

Bassani, F., 1886. Sui fossili e sull'età degli schisti bituminosi triasici di Besano in Lombardia. Communicazione preliminare. Atti della Società Italiana di Scienze Atti Soc. ital. Sci. nat. Museo civ. Stor. nat. Milano 29, 15–17.

Baur, G., 1887. Ueber den Ursprung der Extremitäten der Ichthyopterygia. Berichte über die Versammlungen des Oberrheinischen Geologischen Vereines 20, 17–20.

Brinkmann, W., 1998. *Sangiorgiosaurus* n. g. - eine neue Mixosaurier-Gattung (Mixosauridae, Ichthyosauria) mit Quetschzähnen aus der Grenzbitumenzone (Mitteltrias) des Monte San Giorgio (Schweiz, Kanton Tessin). N. Jb. Geol. Paläont., Abh. 207, 125–144.

de Buffrénil, V., Mazin, J.M., 1990. Bone histology of the ichthyosaurs: comparative data and functional interpretation. Paleobiology 16, 435–447.

Caldwell, M.W., 1997. Modified perichondral ossification and the evolution of paddle-like limbs in ichthyosaurs and plesiosaurs. J. Vert. Paleont. 17, 534–547.

Caldwell, M.W., 2002. From fins to limbs to fins: limb evolution in fossil marine reptiles. Am. J. Med. Genet. 112, 236–249.

Gross, W., 1934. Die Typen des mikroskopischen Knochenbaues bei fossilen Stegocephalen und Reptilien. Z. Anat. Entwicklungsgesch. 203, 731–764.

Houssaye, A., 2009. Pachyostosis" in aquatic amniotes: a review. Integr. Zool. 4, 325–340.

Hulke, J.W., 1873. Memorandum on some fossil vertebrate remains collected by the Swedish expedition to Spitzbergen in 1864 and 1868, Bihang till K. Svenska Vetenskapsakademiens Handlinger, I. Afdelning IV 9, 1–11.

Kiprijanoff, W., 1881. Studien über die fossilien Reptilien Russlands. I. Theil, Gattung *Ichthyosaurus* König. Mémoires de l'Académie des Sciences de St.-Pétersbourg VIIᵉ Série Tome XXVIII (8), 1–103.

McGowan, C., Motani, R., 2003. Ichthyopterygia. Handbuch der Paläoherpetologie [Handbook of Paleoherpetology] Part 8, 1–173.

Merriam, J.C., 1910. The skull and dentition of a primitive ichthyosaurian from the Middle Triassic. University of California Publications. Bulletin of the Department of Geology 5/24, 381–390.

Motani, R., 1999. Phylogeny of Ichthyopterygia. J. Vert. Paleont. 19, 473–496.

Motani, R., 2000. Is *Omphalosaurus* ichthyopterygian?– A phylogenetic perspective. J. Vert. Paleont. 20, 295–301.

Motani, R., 2005. Evolution of fish-shaped reptiles (Reptilia: Ichthyopterygia) in their physical environments and constraints. Annu. Rev. Earth Planet. Sci. 33, 395–420.

Motani, R., 2010. Warm-blooded "sea dragons"? Science 328, 1361–1362.

Motani, R., Minoura, N., Ando, T., 1998. Ichthyosaurian relationships illuminated by new primitive skeletons from Japan. Nature 393, 255–257.

Müller, J., 2004. The relationships among diapsid reptiles and the influence of taxon selection. In: Arratia, G., Wilson, M.V.H., Cloutier, R. (Eds.), Recent Advances in the Origin and Early Radiation of Vertebrates. Verlag Dr. Friedrich Pfeil, München, pp. 379–408.

Nakajima, Y., 2009. Paleoecology of primitive ichthyopterygians suggested by bone histology, Japan Geoscience Union Meeting 2009. Abstract Issue, B102-012.

Quenstedt, F.A., 1852. Handbuch der Petrefaktenkunde, H. Laupp. Tübingen, 792.

Ricqlès, A.de, Buffrénil, V.de, 2001. Bone histology, heterochronies and the return of tetrapods to life in water: were are we? In: Mazin, J.M., Buffrénil, V.de (Eds.), Secondary Adaptations of Tetrapods to Life in Water. Verlag Dr. Friedrich Pfeil, München, pp. 289–310.

Sander, P.M., 2000. Ichthosauria: their diversity, distribution, and phylogeny. Paläont. Z. 74, 1–35.

Sander, P.M., Faber, C., 2003. The Triassic marine reptile *Omphalosaurus*: osteology, jaw anatomy, and evidence for ichthyosaurian affinities. J. Vert. Paleont. 23, 799–816.

Scheyer, T.M., Klein, N., Sander, P.M., 2010. Developmental palaeontology of Reptilia as revealed by histological studies. In: Sánchez-Villagra, M.R. (Ed.), Developmental Vertebrate Palaeontology. Semin. Cell Dev. Biol., 21, pp. 462–470.

Seitz, A.L.L., 1907. Vergleichende Studien über den mikroskopischen Knochenbau fossiler und rezenter Reptilien, und dessen Bedeutung für das Wachstum und Umbildung des Knochengewebes im allgemeinen. Nova Acta, Abh. der Kaiserl. Leop.-Carol. Deutschen Akademie der Naturforscher 87, 230–370.

Walker, J.D., Geissman, J.W., 2009. (Compilers). Geologic Time Scale: Geological Society of America, doi:10.1130/2009.CTS004R2C© 2009. The Geological Society of America.